THE JOURNAL OF BIOLOGICAL CHEMISTRY
Vol. 276, No. 8, Issue of February 23, pp. 5432–5437, 2001
Printed in U.S.A.

Human Glutathione Transferase T2-2 Discloses Some Evolutionary Strategies for Optimization of the Catalytic Activity of Glutathione Transferases*

Received for publication, April 4, 2000, and in revised form, October 6, 2000
Published, JBC Papers in Press, October 23, 2000, DOI 10.1074/jbc.M002818200

Anna Maria Caccuri‡§, Giovanni Antonini§¶‖, Philip G. Board, Jack Flanagan**, Michael W. Parker‡‡, Roberto Paolesse§§, Paola Turella‡‖, Gareth Chelvanayagam**, and Giorgio Ricci‡¶¶‖‖**

*From the ‡Department of Biology, University of Rome "Tor Vergata," 00133 Rome, the ¶Department of Basic and Applied Biology, University of L'Aquila, 67010 L'Aquila, the ‖Department of Biochemical Sciences, University of Rome "La Sapienza," 00185 Rome, Italy, the **Molecular Genetics Group, John Curtin School of Medical Research, Australian National University, Canberra 2601, Australia, ‡‡The Ian Potter Foundation Protein Crystallography Laboratory, St. Vincent's Institute of Medical Research, Fitzroy, Victoria 3065, Australia, the §§Department of Chemical Science and Technology, University of Rome "Tor Vergata," 00133 Rome, and the ¶¶Children's Hospital IRCCS "Bambin Gesù," 00165 Rome, Italy*

Steady state, pre-steady state kinetic experiments, and site-directed mutagenesis have been used to dissect the catalytic mechanism of human glutathione transferase T2-2 with 1-menaphthyl sulfate as co-substrate. This enzyme is close to the ancestral precursor of the more recently evolved glutathione transferases belonging to Alpha, Pi, and Mu classes. The enzyme displays a random kinetic mechanism with very low k_{cat} and $k_{cat}/K_{m(GSH)}$ values and with a rate-limiting step identified as the product release. The chemical step, which is fast and causes product accumulation before the steady state catalysis, strictly depends on the deprotonation of the bound GSH. Replacement of Arg-107 with Ala dramatically affects the fast phase, indicating that this residue is crucial both in the activation and orientation of GSH in the ternary complex. All pre-steady state and steady state kinetic data were convincingly fit to a kinetic mechanism that reflects a quite primordial catalytic efficiency of this enzyme. It involves two slowly interconverting or not interconverting enzyme populations (or active sites of the dimeric enzyme) both able to bind and activate GSH and strongly inhibited by the product. Only one population or subunit is catalytically competent. The proposed mechanism accounts for the apparent half-site behavior of this enzyme and for the apparent negative cooperativity observed under steady state conditions. These findings also suggest some evolutionary strategies in the glutathione transferase family that have been adopted for the optimization of the catalytic activity, which are mainly based on an increased flexibility of critical protein segments and on an optimal orientation of the substrate.

Human glutathione transferase T2-2 (hGSTT2-2, Theta class) is thought to be directly descended from the ancestral precursor of the more recently evolved GSTs[1] found widely expressed in humans (1, 2). All members of the GST superfamily catalyze the nucleophilic addition of GSH to a variety of electrophilic compounds, many with carcinogenic and toxic properties, thus favoring their excretion (3, 4). Human cytosolic GSTs have been grouped into at least five gene-independent classes named Alpha, Pi, Mu, Theta, and Zeta, which differ in their co-substrate and inhibitor specificity as well as in antibody reactivity (3–5). Despite low sequence homology, all of these isoenzymes have very similar three-dimensional structures and very similar topography of the G-site (6–9). The hGSTT2-2 is a homodimeric protein characterized by an additional 40 odd residues at the C terminus and by a peculiar sulfatase reaction (8) not found in the more recently evolved Alpha, Pi, and Mu GSTs. The C-terminal extension, comprising two helices connected by a long loop, completely buries the substrate-binding pocket and occludes most of the GSH-binding site. By virtue of the extension being wedged into the active site, mobile regions found in other GSTs such as helices α2 and α4 are no longer very flexible. In the accompanying paper (10), we have reported that hGSTT2-2 binds GSH with a mechanism different and less efficient than that observed in the other transferases (11, 12), suggesting an evolutionary strategy adopted by the GST family to optimize this process. In this paper we dissect the catalytic mechanism of hGSTT2-2 by means of steady state and pre-steady state kinetic experiments and site-directed mutagenesis. Most of the kinetic studies have been carried out using 1-menaphthyl sulfate (Msu) as co-substrate. A few experiments utilized 1-chloro-2,4-dinitrobenzene (CDNB), one of the best co-substrates for the Alpha, Pi, and Mu GSTs but which was previously considered not to be a substrate for the Theta enzyme (13). The crystallographic studies demonstrated that the crystals were catalytically active in that they could convert the sulfatase substrate, Msu, into the corresponding GSH conjugate with cleavage of the sulfate group. Surprisingly, there was no evidence that the C-terminal extension moves away from the active site, and it was suggested that a narrow tunnel might widen to allow the passage of substrates

* This work was supported by the Italian Ministry of University and Scientific and Technological Research Grant MURST (60%) and MURST PRIN (40%) (to G. R.) and by National Research Council of Italy Grant (Target Project on Biotechnology) (to G. R. and G. A.). The costs of publication of this article were defrayed in part by the payment of page charges. This article must therefore be hereby marked "*advertisement*" in accordance with 18 U.S.C. Section 1734 solely to indicate this fact.

§ Both authors equally contributed to this work.
‖‖ To whom correspondence should be addressed: Dept. of Biology, University of Rome "Tor Vergata," Viale della Ricerca Scientifica, 00133 Rome, Italy. Tel.: 39 6 72594379; Fax: 39 6 2025450; E-mail: riccig@uniroma2.it.

[1] The abbreviations used are: GST, glutathione transferase; Msu, 1-menaphthyl sulfate; CDNB, 1-chloro-2,4-dinitrobenzene, FDNB, 1-fluoro-2,4-dinitrobenzene; SVD, singular value decomposition.

and products between the active site and the surrounding solvent. In accordance with these data, all kinetics reported here depict a somewhat primordial catalysis that is rate-limited by the product release in the case of Msu and by a less than optimal chemical step in the case of CDNB. Recently, two kinetic studies on the rat T2-2 enzyme have been published (14, 15). In those papers, a hysteretic mechanism has been proposed that involves at least three or four different interconverting enzyme conformers. A different kinetic scenario is described here for the human isoenzyme that displays a peculiar half-site catalysis due to a slow or absent interconversion between two catalytically distinct enzyme populations (or active sites).

EXPERIMENTAL PROCEDURES

Reagents and Enzyme Preparation—Msu was synthesized as described by Clapp and Young (16). GSH, *S*-hexylglutathione, CDNB, and 1-fluoro-2,4-dinitrobenzene (FDNB) were Sigma products. His-tagged recombinant hGSTT2-2 and R107A mutant were expressed in *Escherichia coli* and purified using immobilized metal ion chromatography on a nickel-nitrilotriacetic acid matrix (Qiagen) as described previously (13, 17).

Steady State Kinetic Experiments—Kinetic experiments were carried out at 37 °C in 1 ml of carbonate/phosphate/acetate (50:50:50 μM) buffer (Buffer A) at suitable pH values (between pH 5.0 and pH 10.0), containing variable amounts of GSH (from 0.2 to 100 mM) with fixed and saturating Msu concentration (0.25 mM); the reaction was started by the addition of suitable amounts of hGSTT2-2 or of R107A mutant. The reaction rates were measured spectrophotometrically at 298 nm and at 0.1-s intervals for a total period of 120 s. Initial rates were determined by linear regression analysis. Spontaneous reaction was negligible at all the pH values investigated. Data of velocity *versus* [S] were analyzed by a rectangular hyperbole equation to yield V_{max} and K_m values for GSH. The Hill equation was evaluated for possible cooperativity. The activity of hGSTT2-2 with CDNB or FDNB was assayed at constant co-substrate concentration (1 mM) and variable GSH concentration in 0.1 M potassium phosphate buffer, pH 6.5, 37 °C.

Pre-steady State Kinetic Experiments—Rapid kinetic experiments were performed on a Applied Photophysics Kinetic spectrometer stopped-flow instrument equipped with a 1-cm light path observation chamber thermostatted at 37 °C. In a typical experiment, hGSTT2-2 or R107A mutant (30 μM), in Buffer A at a suitable pH value, was rapidly mixed with an identical volume of GSH (10 mM) and Msu (0.5 mM) dissolved in the same buffer. The reaction was followed at 298 nm and performed in the 5–10 pH range. Data were fitted to Scheme I,

$$E + \mathrm{S} \overset{k_1}{\Longrightarrow} E\mathrm{P} \overset{k_2}{\Longrightarrow} E + \mathrm{P}$$

SCHEME I

where E is enzyme, S is substrate, and P is product. Acidic constants for the native enzyme were calculated by fitting kinetic data to Equation 1,

$$y = y_{\lim}(10^{-\mathrm{p}K_{a}1} \times 10^{-\mathrm{pH}})/[(10^{-\mathrm{p}K_{a}1} \times 10^{-\mathrm{p}K_{a}2}) + (10^{-\mathrm{p}K_{a}1} \times 10^{-\mathrm{pH}}) + 10^{-2\mathrm{pH}}] \quad \text{(Eq. 1)}$$

and for R107A mutant by utilizing Equation 2,

$$y = y_{\lim}/(1 + 10^{(\mathrm{p}K_{a} - \mathrm{pH})}) \quad \text{(Eq. 2)}$$

Moreover, pre-steady state kinetics at different GSH concentrations were performed by rapid mixing of the native enzyme (30 μM) dissolved in buffer A, pH 7.0, with the same volume of buffer containing Msu (0.5 mM) and different amounts of GSH from 0.12 to 20 mM. Data were fitted to Scheme II,

$$E + \mathrm{S} \underset{k_{\mathrm{off}}}{\overset{k_{\mathrm{on}}}{\Longleftrightarrow}} E - \mathrm{S} \overset{k_1}{\Longrightarrow} E - \mathrm{P} \overset{k_2}{\Longrightarrow} E + \mathrm{P}$$

SCHEME II

SVD Analysis of the Catalyzed Reaction of GSH with Msu—In a typical experiment, hGSTT2-2 (30 μM), dissolved in Buffer A, pH 7.0, was rapidly mixed with GSH (4 mM) and Msu (0.2 mM) dissolved in the same buffer at 37 °C. 200 points were collected on a faster time base and successively another 200 points were collected on a slower time base. Time-dependent spectra were reconstructed from single wavelength observations (between 240 and 320 nm) by repetitively changing the wavelength following different reagent mixing steps; a 2-nm increment step and 6-nm bandwidth were utilized.

Optical deconvolution of time-dependent spectra sets were performed by means of the software MATLAB (MathWorks, South Natick, MA), running on an Intel Pentium-based personal computer by using singular value decomposition (SVD) in combination with curve fitting algorithms. The matrix of time-dependent spectra (A) is decomposed by SVD into the product of three matrices, $A = UXSXV^T$, where the U columns are the basis spectra, and their time dependence is represented by the V columns. The diagonal values of the S matrix yield the relative occupancies of the basis spectra in the data set. If a data set is contributed by more than one optical transition, deconvolution of the optical components (provided they have different time courses) can be achieved by simultaneously fitting the chosen V columns subset to the kinetic Scheme III (see below). Such best fit of the experimental data to Scheme III, performed using either the program FACSIMILE (AEA, Harwell, UK) or the program GEPASI 3.21 (18–20), obtaining essentially identical results in both cases, has been carried out by means of numerical integration, at variable steps, of the ordinary differential equations according to Scheme III. The resulting matrix of the time dependences of the molar fraction of the intermediate species can be used to reconstruct (from the experimental matrix of time-dependent spectra) the spectra of the intermediate species at different times after mixing (21–23).

RESULTS AND DISCUSSION

Steady State Kinetics of hGSTT2-2 with Msu as Co-substrate—Steady state kinetics of hGSTT2-2 has been analyzed at fixed and saturating Msu concentrations (0.25 mM) and variable GSH concentrations between 0.2 and 100 mM. Experiments were performed at 37 °C and at different pH values between pH 5.0 and 10.0. The dependence of velocity on GSH concentration does not obey the Michaelis-Menten equation, and hGSTT2-2 displays apparent negative cooperativity toward GSH as though the binding of GSH to the first subunit induces a lowering of affinity in the empty subunit. Hill plots, obtained from experiments at various pH values, yield a Hill coefficient ranging from 0.7 to 0.8. This non-Michaelian kinetic behavior is unexpected as the isothermal binding of GSH has been found to be hyperbolic (10). Thus, this may correspond to a true cooperativity only if the presence of the co-substrate in the active site causes an intersubunit communication that is absent without it. Due to the very high affinity for Msu (K_m = 5 μM), it is unclear if hGSTT2-2 displays a cooperative behavior toward this co-substrate. For the sake of simplicity, kinetic data, at variable GSH concentration between 0.2 and 4 mM, were only considered. They can be fit satisfactory to a simple hyperbolic equation that gives a rough estimate of the apparent $K_{m(\mathrm{GSH})} \cong 0.5$ mM. This value does not change between pH 5.0 and pH 9.0, showing an increase only at higher pH values. k_{cat} value, calculated at 100 mM GSH, is low (0.15 s^{-1} at pH 7.0) and scarcely pH-dependent between pH 5.0 and pH 8.0 (Fig. 1*A*). Under more alkaline conditions, k_{cat} value increases, reaching a 5-fold increase at pH 10. At this pH, the enzyme is unstable, and in a few minutes it inactivates irreversibly. Secondary plots of $1/k_{cat}$ and K_m/k_{cat} in the presence or absence of the enzymatic product GS-Msu (data not shown) suggest that hGSTT2-2 follows a rapid equilibrium random mechanism like the rat isoenzyme (14).

As a whole, several aspects seem to characterize the hGSTT2-2 steady state kinetics when compared with other human GSTs as follows: (*a*) very low (at least 100-fold lower) k_{cat} and $k_{cat}/K_{m(\mathrm{GSH})}$ values; (*b*) the apparent negative cooperativity, also observed in the Alpha and Mu GSTs, but in those enzymes it is probably the consequence of a steady state random kinetic mechanism (24); (*c*) k_{cat} value is pH independent, whereas in human Alpha, Mu, and Pi GSTs (with CDNB as co-substrate) it parallels the deprotonation of the bound GSH (11, 25, 26).

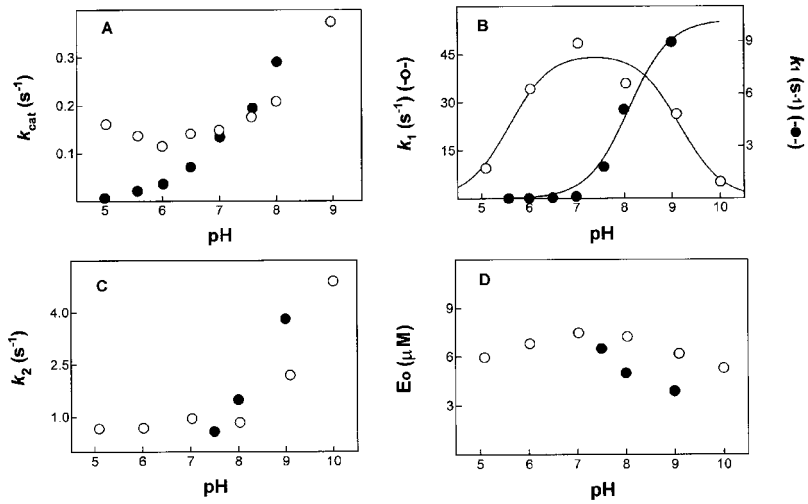

FIG. 1. **Effect of pH on kinetic parameters.** *A,* pH dependence of k_{cat} (calculated 10 s after mixing) for hGSTT2-2 (○) and for R107A mutant (●); experiments were performed at 37 °C as reported under "Experimental Procedures." The pH dependence of the pseudo-first order kinetic constant for product formation (k_1) (*B*), of the first order kinetic constant for product release (k_2) (*C*), and of the active enzyme concentration (E_0) (*D*) are obtained by stopped-flow experiments with hGSTT2-2 (○) and with R107A mutant (●). The *solid lines* in *B* are the best fit of experimental data to Equation 1 (native enzyme) and to Equation 2 (R107A mutant).

Pre-steady State Kinetics—Pre-steady state kinetics of hGSTT2-2 have been dissected by means of stopped-flow experiments performed at pH 7.0 and 37 °C. Representative time courses of the enzymatic reaction, obtained at variable GSH concentrations (from 0.06 to 10 mM) and in the presence of saturating Msu (0.25 mM), are shown in Fig. 2*B*. The early stage of catalysis shows a well defined burst phase of product accumulation followed by a slower, linear phase that corresponds to the product release. The slower portion is almost independent on GSH concentration indicating that the product release occurs at the maximum rate even at low GSH concentrations. The best fit of these kinetic data to the minimal Scheme II (see "Experimental Procedures") yields apparent microscopic rate constants reported in Table I. It appears that k_{on} and k_{off} are close to those previously found for the formation of the binary complex *E*-GSH (10). Thus, the presence of Msu does not affect the binding of GSH, and this co-substrate interacts with the active site at a higher or similar velocity compared with GSH.

When the linear phase following the burst is extrapolated back on the *y* axis, the intercept (π) yields the effective active enzyme concentration, according to $\pi = [E]_0 (k_1/(k_1 + k_2))^2$. In the case of hGSTT2-2, E_0 corresponds to only about 50% of the total enzyme used. This sub-stoichiometric amount of active enzyme has been confirmed by replicate experiments with different enzyme batches, and it seems to be a peculiarity of the human Theta isoenzyme. A second unusual finding is that k_{cat} calculated above by conventional spectrophotometry (0.15 s^{-1}), if normalized to the effective active enzyme concentration, is 3-fold lower than k_2 (1 s^{-1}). By using longer acquisition times in the stopped flow apparatus (a few seconds after mixing), the rate of product release decreases, so that k_2 approaches k_{cat}. In other words, the experimental traces given by the stopped-flow apparatus are now comparable to those observed in the conventional spectrophotometer. Thus, after the burst phase that is related to k_1, two subsequent phases characterize the steady state kinetic behavior of T2-2. The first one occurs within 1–1.5 s after mixing (Fig. 2*B*); the slower second phase is visible at longer acquisition times (see Fig. 2, *A* and *C*).

pH Dependence of Kinetic Parameters—The pH dependence of the pre-steady state kinetics has been studied between pH 5.0 and 10.0 at fixed GSH (5 mM) and Msu (0.25 mM) concentrations. Data were analyzed according to Scheme I (see "Experimental Procedures"). Fig. 1 shows the pH dependence of the pseudo-first order rate constant for product formation (k_1) and for the first order rate constant for product release (k_2) and the pH dependence of the enzyme concentration (E_0) calculated from the π amplitude. Whereas E_0 corresponds to about 50% of the total protein between pH 5.0 and pH 9.0 (Fig. 1*D*), the pH dependence of k_1 shows a large bell-shaped trend (Fig. 1*B*). The best fit of the experimental data to Equation 1 yields an apparent $pK_{a1} = 5.6 \pm 0.20$ and $pK_{a2} = 9.2 \pm 0.20$. pK_{a1} is close to the apparent pK_a of the bound GSH ($pK_a = 6.1$), as calculated in the binary complex (10). The presence of Msu in the active site probably causes a more favorable deprotonation of the bound GSH. The decrease of k_1 above pH 8.0 suggests that at least one protonated residue, with an apparent pK_a of 9.2, is involved in optimizing the orientation of the substrate(s) for the chemical step. k_2, which has been calculated within 1 s after mixing, follows a trend similar to that of k_{cat}, *i.e.* is pH independent up to pH 8.0, showing a remarkable increase only above pH 9.0 (Fig. 1*C*). The crystal structure of the Msu complex provides an explanation as to why the product release is rate-limiting; the menaphthyl ring is firmly wedged in the H-site with the C-terminal extension completely blocking access to the surrounding solvent. The Msu complex crystal structure was examined with a view to understanding why product release is greatly accelerated above pH 9. No candidate residues were identified that might be involved in loosening the contacts of the C-terminal extension from the rest of the protein. However, a number of residues were identified in the narrow tunnel that leads from the active site. These residues include His-40, Lys-41, Lys-53, Glu-66, Asp-104, and Cys-105. In addition to these residues, the α-amino group of GSH is another candidate. In each case the residue is in a microenvironment that might sufficiently disturb its pK_a to cause the pH-dependent kinetic effect. In summary, the kinetic data support the previous hypothesis that the C-terminal extension does not move to allow the passage of substrates and products, but instead a small tunnel acts as the gateway (8).

Effect of Arg-107 Mutation on Catalysis—In the structure of the Msu complex, Arg-107 interacts with both GSH and the cleaved sulfate ion (8). In the accompanying paper (10), Arg-107 has been shown to play a crucial role in the activation of GSH since mutating this residue causes the pK_a of the thiolate anion to shift from 6.1 to 7.8. Steady state kinetics is also modified. For example, between pH 5.0 and pH 8.0, k_{cat} shows a pH dependence that contrasts with the pH invariance of the native enzyme (Fig. 1*A*). Stopped-flow experiments demonstrate a well defined burst phase only above pH 7.0, although it is completely absent under more acidic conditions. This means that below pH 7.0, the chemical event becomes too slow, and the product does not accumulate. The pH dependence of k_1 displays an apparent pK_a of 8.1 (Fig. 1*B*), a value close to the

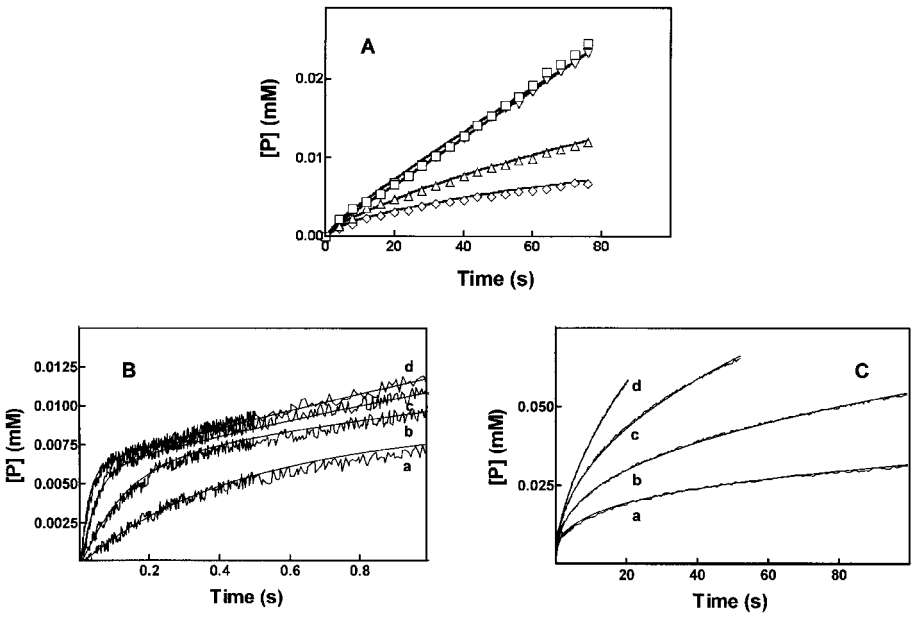

FIG. 2. **Time course of the GS-Msu product formation.** *A,* steady state kinetics of hGSTT2-2 (2 μM) performed at pH 7.0 and 37 °C in the presence of Msu (0.25 mM) and variable GSH concentrations: 0.2 mM (◇), 1 mM (Δ), 10 mM (▽) and 100 mM (□). *B,* stopped-flow kinetics of hGSTT2-2 (15 μM) performed at pH 7.0 and 37 °C in the presence of Msu (0.25 mM) and variable GSH concentrations: 0.1 mM (*a*), 0.3 mM (*b*), 1 mM (*c*), and 3 mM (*d*). *C,* stopped-flow kinetics of hGSTT2-2 at longer acquisition times (up to 100 s); experimental conditions as in *B*. The *solid lines* are obtained by the simultaneous fitting of pre-steady and steady state kinetic data to Scheme III.

TABLE I
Stopped-flow kinetic parameters have been calculated by fitting pre-steady state kinetic data at variable GSH concentrations to Scheme II

k_{on}	$(3 \pm 1) \times 10^4$ M^{-1} s^{-1}
k_{off}	41 ± 8 s^{-1}
k_1	50 ± 20 s^{-1}
k_2	0.6 ± 0.15 s^{-1}

TABLE II
Stopped-flow kinetic parameters have been calculated by fitting pre-steady state, steady state kinetic data, and binding data (10) to Scheme III

k_{on}	$(2.9 \pm 1) \times 10^4$ M^{-1} s^{-1}
k_{off}	34 ± 9 s^{-1}
k_1	83 ± 5 s^{-1}
k'_1	0.8 ± 0.1 s^{-1}
k_2	1 ± 0.4 s^{-1}
k_{-2}	$(15 \pm 3) \times 10^5$ M^{-1} s^{-1}
E:E'	41:59

pK_a of GSH in the binary complex with this mutant (10). Thus, the replacement of Arg-107 yields a similar shift of pK_a both in the binary and in the ternary complexes of hGSTT2-2.

It is likely that the protonated form of Arg-107 plays a role in the chemical step by promoting not only the GSH ionization but also a proper orientation of the substrate. In fact, in the native enzyme, when GSH and Arg-107 are in the ionized form (between pH 7.0 and 8.0), k_1 reaches the limiting value of about 45 s^{-1}. Conversely, the limiting value of k_1 in R107A under alkaline conditions is only 10 s^{-1}. This value is close to that obtained in the native enzyme at pH 10 when Arg-107 is almost uncharged, and the bound GSH is fully deprotonated.

The slight increase of k_{cat} and k_2 in the mutant under alkaline conditions also suggests that replacement of Arg-107 may facilitate the product release (Fig. 1, *A* and *C*). It was previously reported that mutation of Arg-107 had a detrimental effect on the sulfatase reaction measured in Tris/HCl, pH 8.3 (17). Conversely, under alkaline conditions, we found a comparable or even higher activity of the Y107A mutant compared with the wild type enzyme. This may be probably due to the presence, in the buffers utilized, of phosphate which appears to stabilize the Y107A mutant in a more active conformation.

A Proposed Mechanism for hGSTT2-2—A minimal kinetic mechanism that accounts for all pre-steady state and steady state kinetic data is reported in Scheme III. This involves two enzyme populations E and E' (slowly or not interconverting and each representing about 50% of the total population) both able to bind and activate GSH but just one competent for a fast catalytic event. The product formation occurs in E at a rate about 100 times faster than it occurs in E'. Product is slowly released from both E and E', whereas it enters at a high rate resulting in a relevant enzyme inhibition. Table II shows the microscopic rate constants calculated by a global fit of all pre-steady state and steady state kinetic data and GSH binding data to the proposed mechanism. The best fit of the experimental data to Scheme III superimpose well the experimental traces (see Fig. 2) in the large temporal window of 0.001–100 s. The proposed kinetic mechanism accounts for the apparent half-site behavior found in the pre-steady state analysis and also for the apparent cooperativity observed under steady state conditions. This mechanism is compatible either with the existence of two slowly interconverting enzyme populations or with a single dimer population having one subunit more active than the other. Actually, there are extensive contacts in the dimer interface, particularly at the base of the molecule where there are numerous hydrophobic interactions. In comparison to other GSTs the interface is much more extensive and includes the helical towers of the C-terminal domain and the C-terminal tails. These latter elements also form walls of the H-sites (8). It is thus quite conceivable that communication could exist between the active sites, and this could be the base for a true half-site catalysis as a result of a strong negative cooperativity.

$$E + S \underset{k_{off}}{\overset{k_{on}}{\rightleftharpoons}} ES \overset{k_1}{\Rightarrow} EP \underset{k_{-2}}{\overset{k_2}{\rightleftharpoons}} E + P$$

$$\Updownarrow \text{ slow}$$

$$E' + S \underset{k_{off}}{\overset{k_{on}}{\rightleftharpoons}} E'S \overset{k'_1}{\Rightarrow} E'P \underset{k_{-2}}{\overset{k_2}{\rightleftharpoons}} E' + P$$

SCHEME III

SVD Analysis of the Catalyzed Reaction of GSH with Msu—The proposed mechanism has been supported by examining the time dependence of intermediate species (E, E', ES, $E'S$, EP, $E'P$, and P) along the catalytic pathway. This has been obtained by SVD analysis and best fit of the experimental data to Scheme III as described under the "Experimental Procedures." Fig. 3*A* depicts the temporal evolution of the difference spectra

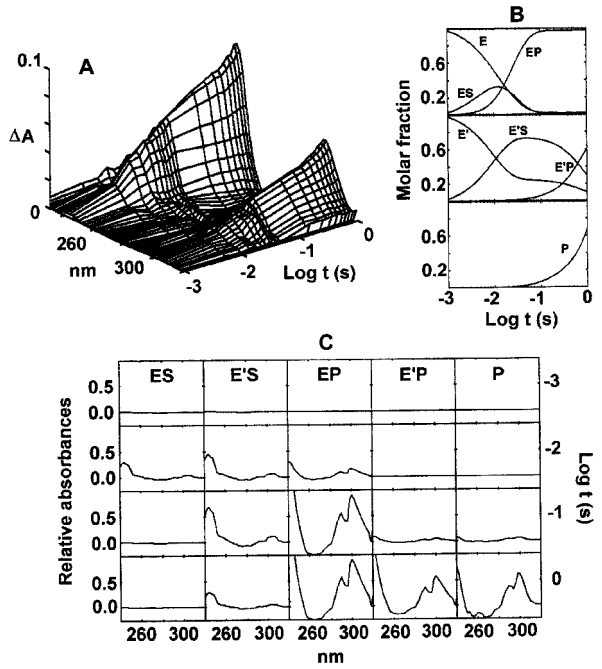

FIG. 3. **SVD analysis of the catalyzed reaction between GSH and Msu.** *A,* the temporal evolution (from 0.001 to 1 s) of the difference spectrum of the reaction mixture is shown. The spectrum was obtained by subtracting the first spectrum, recorded 1 ms after mixing (less than 2–3% of the total burst reaction). *B* shows the time courses of the species *E*S, *E*′S, *E*P, *E*′P, and P obtained as reported under "Experimental Procedures," according to the minimal reaction Scheme III. Differential spectra of the optical species were then reconstructed at different times after mixing and are reported in *C*.

(in the range 240–320 nm) obtained after rapid mixing hGSTT2-2 with GSH and Msu. These data, subjected to SVD analysis, were best fit to the proposed Scheme III, employing the microscopic rate constants listed in Table II. The time dependences of the molar fraction of the intermediate species are reported in Fig. 3*B*. It is also possible to reconstruct the spectrum of each intermediate species at a given time. Fig. 3*C* shows representative spectral sets at 0.001, 0.01, 0.1, and 1 s. It can be noted that both *E*S and *E*′S are characterized by a peak below 250 nm (the intrinsic instrumental limit did not allow us to follow accurately any optical transition below 250 nm), which may be due to the GSH thiolate. On the contrary, the *E*P and *E*′P species show a double peak with a maximum at about 300 nm, which might correspond to the product (P) as it overlaps the spectrum of synthetic GS-Msu adduct (data not shown).

It is useful now to look at the relative amount of the different species and their spectral contribution during the approach to the steady state phase. *E*S and *E*′S formation is synchronous (in the millisecond time scale) to the GSH-binding event. However, *E*S reaches a maximum (about 20% of the total) 10 ms after mixing, and it is absent at 100 ms when *E*P is the prevalent species. *E*′S reaches a maximum (about 70% of the total) after 30 ms, and it is still present (about 20%) at 1 s after mixing. *E*P appears early, reaches a maximum after 100 ms and then remains populated at about 95% during the steady state phase. *E*′P is slowly formed only after 100 ms and reaches a maximum after 1 s. The product release (P) starts only after 50–100 ms and increases during the steady state phase.

As a whole, this analysis represents a time-dependent spectral visualization of the proposed mechanism and adds new elements to the traditional kinetic analysis. The good overlap of the deconvoluted spectra with those of the separate species is an intrinsic control of the correct fit of kinetic data to Scheme III.

CDNB as Substrate—Despite previous reports (13) in our experimental conditions, we found that hGSTT2-2 has a small but detectable activity with CDNB, one of the best co-substrates for Alpha, Pi, and Mu GSTs. The presence of phosphate seems to be crucial for this activity, and at pH 6.5 and 37 °C, hGSTT2-2 displays a k_{cat} value of 0.07 s^{-1} and a $K_{m(GSH)}$ of about 0.6 mM. Thus its catalytic efficiency, k_{cat}/K_m, may be estimated to be 100 s^{-1} M^{-1}, about 1000 times lower than values obtained for the recently evolved GSTs. Pre-steady state kinetic experiments did not reveal any product accumulation before the steady state attainment, so the rate-limiting step in catalysis would be the chemical event or a preceding conformational transition of the ternary complex (27). By replacing CDNB with its fluoro-analogue, FDNB, k_{cat} increases 40 times. Since spontaneous reaction between FDNB and GSH is 38 times faster than that with CDNB, the chemical step is a reasonable candidate as rate-limiting in catalysis. It is well known that this nucleophilic aromatic substitution occurs via an addition-elimination sequence that involves a short-lived σ-complex (27). As fluoride is a poorer leaving group than chloride but enhances the electrophilic propensity of the C-1 atom, the σ-complex formation seems to be the rate-contributing event in hGSTT2-2 catalysis with CDNB. The remarkable increase of k_{cat} with FDNB also indicates that the energy barrier due to a physical event in the catalytic pathway (product release or structural transition) must be much lower than that of the chemical step.

Concluding Remarks—This paper presents a series of investigations to dissect the hGSTT2-2 catalytic mechanism, which is complicated by some unusual kinetic properties of this enzyme. A multidisciplinary approach has been found essential to reach a reasonable kinetic model; all steady state and pre-steady state kinetic data reported here are fit well to the kinetic mechanism of Scheme III. Even if more complicated scenarios are also plausible, this mechanism accounts for the apparent negative cooperativity, the apparent half-site behavior of hGSTT2-2, and the peculiar kinetic trend observed in the early stage of catalysis. Arg-107 is crucially involved in GSH activation and in a proper orientation of GSH for catalysis. The protonation of the guanidine side chain is an essential requirement for its contributing role.

In addition, the SVD analysis supports the proposed mechanism giving a reasonable spectral visualization of the species occurring along the kinetic pathway.

Apart from the obvious interest in elucidating an unusual kinetic mechanism, our data also present an opportunity to compare an enzyme from an "old" GST family like hGSTT2-2 to the "younger" Alpha, Pi, and Mu class GSTs. One crucial difference resides in the structural rigidity of the hGSTT2-2 that may be the origin of most of the kinetic oddities described above. A comparison of the mobility profile of representative GST isoenzymes has been presented in the accompanying paper (10). This comparison demonstrates the relative rigidity of the primordial enzyme compared with the more recently evolved GSTs and, in particular, the absence of a sequence of "cold" and "hot" regions along the polypeptide chain. Recently, molecular dynamics simulation data on GSTP1-1 (Pi class) revealed that segmental motions of the protein may play a crucial role in catalysis. GSTP1-1 behaves as a "dancing" enzyme with a breathing involving the helix α2 region and other protein segments that produce a fast alternate opening and closing of the active site (28, 29). A dynamic fluorescence study also indicated GSTP1-1 exists as two families of rapidly interconverting conformers with different binding properties (30). The interconversion is, however, very fast (with times slower than nanoseconds but much faster than milliseconds), so that

any half-site behavior or sub-stoichiometric working active sites has not been observed. Similarly, in the human A1-1 GST (Alpha class), a rapid transition has been proposed involving motions of the flexible C-terminal segment that partially covers the G-site (31). Even the Mu class GST, where the active site is confined by two flexible loops, may display a similar fluctuating accessibility (32). On the whole, it appears that the very similar flexibility profiles found in Alpha, Pi, and Mu GSTs (10) are not incidental but reflect a precise evolution strategy to enhance the catalytic efficiency of the GST superfamily. How did GSTs evolve toward a more flexible structure? The partial or total deletion of a cumbersome segment like the C-terminal extension of hGSTT2-2, is one possibility, even though it causes a loss of the sulfatase activity. Replacement of crucial residues involved in electrostatic interactions may be a second possibility. For example, Arg-107 is likely involved in an electrostatic interaction with Asp-104, and its replacement by Ala induces an increased flexibility of the active site causing an improvement of the GSH-binding properties (10). This mutation also favors the release of product as evidenced by the slightly higher values of k_2 of the mutant (see Fig. 1). However Arg-107 is crucially involved in the proper orientation and activation of GSH, so it was strictly conserved during the natural intra-class evolution of this enzyme.

What we found for the hGSTT2-2 catalysis using a small co-substrate like CDNB also indicates that other evolutionary targets may have been pursued. In fact the chemical event is largely rate-limiting in the CDNB case; the active site is rather large and a small substrate like CDNB could not be optimally orientated in such a site. The optimization in catalysis could be achieved by a refinement of the substrate orientation in the active site.

Acknowledgment—We thank Prof. M. Coletta for helpful discussions.

REFERENCES

1. Pemble, S. E., and Taylor, J. B. (1992) *Biochem. J.* **287,** 957–963
2. Pemble, S. E., Wardle, A. F., and Taylor, J. B. (1996) *Biochem. J.* **319,** 749–754
3. Armstrong, R. N. (1997) *Chem. Res. Toxicol.* **10,** 2–18
4. Salinas, A. E., and Wong, M. G. (1999) *Curr. Med. Chem.* **6,** 279–309
5. Board, P. G., Baker, R. T., Chelvanayagam, G., and Jermiin, L. S. (1997) *Biochem. J.* **328,** 929–935
6. Dirr, H. W., Reinemer, P., and Huber, R. (1994) *Eur. J. Biochem.* **220,** 645–661
7. Wilce, M. C. J., and Parker, M. W. (1994) *Biochim. Biophys. Acta* **1205,** 1–18
8. Rossjohn, J., McKinstry, W. J., Oakley, A. J., Verger, D., Flanagan, J., Chelvanayagam, G., Tan, K.-L., Board, P. G., and Parker, M. W. (1997) *Structure* **6,** 309–322
9. Wilce, M. C. J., Board, P. G., Feil, S. C., and Parker, M. W. (1995) *EMBO J.* **14,** 2133–2143
10. Caccuri, A. M., Antonini, G., Board, P. G., Flanagan, J., Parker, M. W., Paolesse, R., Turella, P., Federici, G., Lo Bello, M., and Ricci, G. (2001) *J. Biol. Chem.* **276,** 5427–5431
11. Caccuri, A. M., Lo Bello, M., Nuccetelli, M., Nicotra, M., Rossi, P., Antonini, G., Federici, G., and Ricci, G. (1998) *Biochemistry* **37,** 3028–3034
12. Caccuri, A. M., Antonini, G., Board, P. G., Parker, M. W., Nicotra, M., Lo Bello, M., Federici, G., and Ricci, G. (1999) *Biochem. J.* **344,** 419–425
13. Tan, K.-L., Chelvanayagam, G., Parker, M. W., and Board, P. G. (1996) *Biochem. J.* **319,** 315–321
14. Jemth, P., and Mannervik, B. (1999) *Biochemistry* **38,** 9982–9991
15. Jemth, P., and Mannervik, B. (2000) *J. Biol. Chem.* **275,** 8618–8624
16. Clapp, J. J., and Young, L. (1970) *Biochem. J.* **118,** 765–771
17. Flanagan, J. U., Rossjohn, J., Parker, M. W., Board, P. G., and Chelvanayagam, G. (1999) *Protein Sci.* **8,** 2205–2212
18. Mendes, P. (1993) *Comput. Appl. Biosci.* **9,** 563–571
19. Mendes, P. (1997) *Trends Biochem. Sci.* **22,** 361–363
20. Mendes, P., and Kell, D. B. (1998) *Bioinformatics* **14,** 869–883
21. Henry, E. R., and Hofrichter, J. (1992) *Methods Enzymol.* **210,** 129–192
22. Hendler, R. W., and Shrager, R. I. (1994) *J. Biochem. Biophys. Methods* **28,** 1–33
23. Antonini, G., Bellelli, A., Brunori, M., and Falcioni, G. (1996) *Biochem. J.* **314,** 533–540
24. Ivanetich, K. M., Goold, R. D., and Sikakana, C. N. T. (1990) *Biochem. Pharmacol.* **39,** 1999–2004
25. Widersten, M., Björnestedt, R., and Mannervik, B. (1996) *Biochemistry* **35,** 7731–7742
26. Chen, W.-J., Graminski, G. F., and Armstrong, R. N. (1988) *Biochemistry* **27,** 647–654
27. Ricci, G., Caccuri, A. M., Lo Bello, M., Rosato, N., Mei, G., Nicotra, M., Chiessi, E., Mazzetti, A. P., and Federici, G. (1996) *J. Biol. Chem.* **271,** 16187–16192
28. Stella, L., Nicotra, M., Ricci, G., Rosato, N., and Di Iorio, E. (1999) *Proteins* **37,** 1–9
29. Stella, L., Di Iorio, E., Nicotra, M., and Ricci, G. (1999) *Proteins* **37,** 10–19
30. Stella, L., Caccuri, A. M., Rosato, N., Nicotra, M., Lo Bello, M., De Matteis, F., Mazzetti, A. P., Federici, G., and Ricci, G. (1998) *J. Biol. Chem.* **273,** 23267–23273
31. Nieslanik, B. S., Dabrowski, M. J., Lyon, R. P., and Atkins, W. M. (1999) *Biochemistry* **38,** 6971–6980
32. Parsons, J. F., Xiao, G., Gilliland, G. L., and Armstrong, R. N. (1998) *Biochemistry* **37,** 6286–6294

Human Glutathione Transferase T2-2 Discloses Some Evolutionary Strategies for Optimization of the Catalytic Activity of Glutathione Transferases

Anna Maria Caccuri, Giovanni Antonini, Philip G. Board, Jack Flanagan, Michael W. Parker, Roberto Paolesse, Paola Turella, Gareth Chelvanayagam and Giorgio Ricci

J. Biol. Chem. 2001, 276:5432-5437.
doi: 10.1074/jbc.M002818200 originally published online October 23, 2000
